ISSN 0027-1349, Moscow University Physics Bulletin, 2024, Vol. 79, No. 5, pp. 592–595. © Allerton Press, Inc., 2024.
Russian Text © The Author(s), 2024, published in Vestnik Moskovskogo Universiteta, Seriya 3: Fizika, Astronomiya, 2024, Vol. 79, No. 5, 2450402.

OPTICS AND SPECTROSCOPY. LASER PHYSICS

Faraday Rotation Dynamics in Hybrid Magnetophotonic Metasurfaces

A. M. Chernyak[1,2], A. I. Musorin[1,2], and A. A. Fedyanin[2*]

[1] *Department of Materials Science, Shenzhen MSU-BIT University, Shenzhen, 517182 P.R.C.*

[2] *Department of Nanophotonics, Faculty of Physics, Lomonosov Moscow State University, Moscow, 119991 Russia*

Received May 17, 2024; revised June 28, 2024; accepted July 9, 2024

Abstract—The behavior of Faraday rotation on the femtosecond timescale in Mie-resonant magnetophotonic metasurfaces formed by a two-dimensional array of silicon nanodisks coated with a thin nickel film is studied. It is shown that in the static case, the maximum of polarization plane rotation is 14° at the resonant wavelength for spectrally overlapped electric and magnetic dipole modes. When a single femtosecond laser pulse passes through the designed metasurface, it splits into two pulses with durations twice shorter than the original one, and the polarization planes are rotated in opposite directions, forming almost orthogonal replicas.

Keywords: Faraday effect, magneto-optics, Mie resonances, nanophotonics, ultrafast processes

DOI: 10.3103/S002713492470190X

INTRODUCTION

Typically weak magneto-optical (MO) effects can be significantly enhanced by increasing the interaction time of radiation with gyrotropic materials. Optical resonances are an effective approach to achieve this due to strong light confinement inside magnetic media [1]. Materials with large real and small imaginary parts of the refractive index, such as dielectrics and semiconductors, enable radiation to couple to eigenmodes within nanocavities. The resonant light scattering by such nanoparticles makes possible to reproduce effects similar to those observed in plasmonic ones but without the need of complex geometries typically required in the case of metallic structures [2–6]. For instance, it has been shown experimentally and numerically that the excitation of Mie resonances plays a crucial role in enhancing the intensity and polarization MO effects [7–10].

In contrast to continuous radiation sources, laser pulses can exhibit complex polarization dynamics after interaction with a nanostructured medium if the lifetime of the resonance is comparable to the duration of the wave packet [11, 12]. However, such studies in magnetophotonic metasurfaces have not been carried out yet. This work aims to eliminate this gap by performing numerical calculations of the femtosecond dynamics of the Faraday effect in Mie-resonant silicon disks coated with a thin nickel film.

*E-mail: fedyanin@nanolab.phys.msu.ru

1. SAMPLE. STATIC SPECTRA

The finite-difference time-domain (FDTD) method, implemented in Ansys Lumerical FDTD software, is used for the numerical calculations. The problem is solved for a three-dimensional model with periodic boundary conditions along the X and Y axes and perfectly matched layers along the Z direction. Transmittance spectrum is calculated for normal incidence of a plane electromagnetic wave propagating along the Z-axis (Fig. 1a). The polarization is X-oriented. An external magnetic field coincides with the Z direction. To evaluate the magnitude of the Faraday effect, which manifests itself as the polarization plane rotation of linearly polarized light by an angle θ_F when light propagates through a magnetized medium, the real part of the arctangent of the electric field components ratio in the far diffraction zone is considered:

$$\theta_F(\text{deg}) = \frac{180^\circ}{\pi}\text{Re}\left(\arctan\left(\frac{E_y}{E_x}\right)\right). \quad (1)$$

The studied sample is a two-dimensional square lattice of silicon nanodisks with period $P = 400$ nm placed on a quartz substrate. The height of the nanodisks is $H = 145$ nm and the diameter is $d = 280$ nm. These parameters are selected to get optical Mie resonance near the wavelength of 800 nm. The disks and substrate are covered with a 5-hm-thick nickel film (see Fig. 1a). The dispersion of the gyration of the magnetic material is taken into

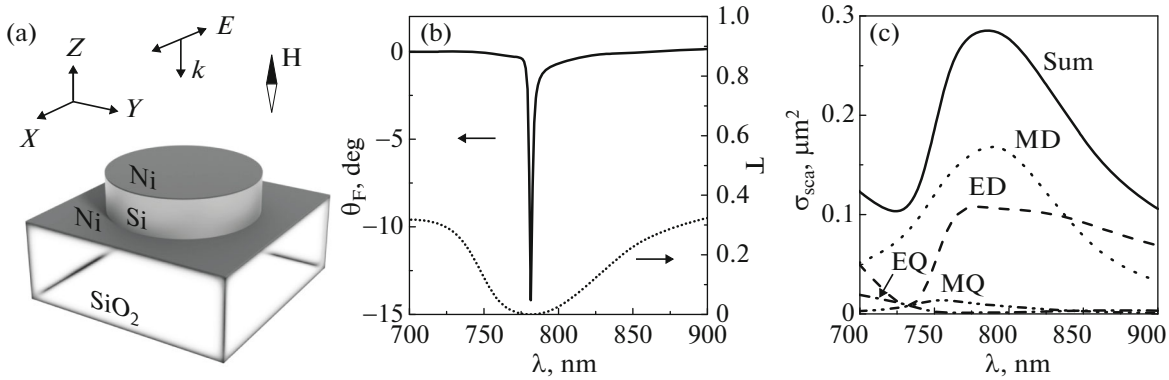

Fig. 1. (a) Schematic representation of a unit cell of the studied metasurface. (b) Numerical calculations of transmittance (dotted curve) and Faraday rotation (solid curve) spectra of the metasurface. (c) Scattering cross section spectra. MD and ED denote the magnetic and electric dipole moments, MQ and EQ are the magnetic and electric quadrupole moments.

account [13]. The applied magnetic field magnitude corresponds to the saturation field [9]. In Fig. 1b, the dotted curve represents the transmittance spectrum of this structure with the resonance feature at the wavelength $\lambda = 782$ nm. To establish its nature, the scattering cross section of the first four fundamental Mie modes is calculated, which gives the main contribution to the spectral range of interest [14]:

$$\sigma_{\text{sca}}(\mu\text{m}^2) \simeq \frac{k_0^4}{12\pi\varepsilon_0^2\mu_0 v_d I_0}\left|\mathbf{p} + \frac{ik_d}{v_d}\mathbf{T}\right|^2 + \frac{k_0^4\varepsilon_d}{12\pi\varepsilon_0 v_d I_0}|\mathbf{m}|^2 + \frac{k_0^6\varepsilon_d}{1440\pi\varepsilon_0^2\mu_0 v_d I_{inc}}\sum_{\alpha\beta}\left|\hat{Q}_{\alpha\beta}\right|^2 + \frac{k_0^6\varepsilon_d^2}{160\pi\varepsilon_0 v_d I_0}\sum_{\alpha\beta}\left|\hat{M}_{\alpha\beta}\right|^2, \quad (2)$$

where $\alpha = x, y, z$ and $\beta = x, y, z$; k_0 and k_d are the wave vectors in vacuum and in the medium; $v_d = c/\sqrt{\varepsilon_d}$ is the light speed in the medium with the dielectric constant ε_d; ε_0, μ_0 are the dielectric and magnetic permittivities of vacuum; I_0 is the intensity of the incident radiation; $\mathbf{p}$, $\mathbf{T}$, and $\mathbf{m}$ denote the electric, toroidal, and magnetic dipole moments, respectively, $\hat{Q}$ and $\hat{M}$ refer to the electric and magnetic quadrupole moments. The contributions of the electric and magnetic dipole resonances are predominant in the total cross section in the vicinity of the wavelength $\lambda = 782$ nm. Higher-order modes can be neglected due to their insignificant influence in this spectral range. Thus, the geometry of the particles leads to a spectral interference of these two modes which manifests itself as a single dip in the transmittance spectrum (see Fig. 1b). The quality factor of the resonance is approximately $\sim$10, which is a typical value for optical Mie resonances [4]. The Faraday rotation spectrum is represented in Fig. 1b by a solid curve. The interference of the local fields of the two excited modes leads to a significant shrinkage of the magneto-optical response and a multiple enhancement of the Faraday effect. A sharp increase in the polarization plane rotation up to the angle $\theta_{\text{F}} = -14°$ is observed under resonance conditions. It exceeds the value of the Faraday rotation of an unstructured nickel film of the same thickness by three orders of magnitude [9]. The resonance quality factor in the magneto-optical response is approximately $\sim$300 estimated by the Fano formula [15]:

$$\theta_F = \left|a_1 + ia_2 + \frac{b}{\omega - \omega_0 + i\gamma}\right|^2, \quad (3)$$

where ω_0 is the central frequency of resonance y, is the attenuation coefficient and a_1, a_2, b are real constants. In other systems this value is around 20 regardless of the resonance type (Mie, local plasmons, propagating plasmon-polaritons) [9, 16, 17]. The maximum value of the Q-factor of the resonance in the Faraday rotation spectrum was reported in [10], where it was of the order of 200. The presented calculations were performed in the stationary case, when the sample is illuminated by a continuous radiation source. In the context of a laser pulse, the relationship between its duration and the resonance lifetime is crucial. Due to the complicated spatial structure of the local electromagnetic field distribution for the case of spectrally overlapped resonances, different Q-factors of the optical and magneto-optical responses, it is of interest to explore the behavior of the polarization plane rotation on the femtosecond scale.

2. FEMTOSECOND DYNAMICS OF FARADAY ROTATION

The propagation of a Gaussian pulse of the electric field with unit amplitude and full width at half maximum $\tau = 240$ fs through the metasurface is modeled for three carrier wavelengths of radiation: 778, 782,

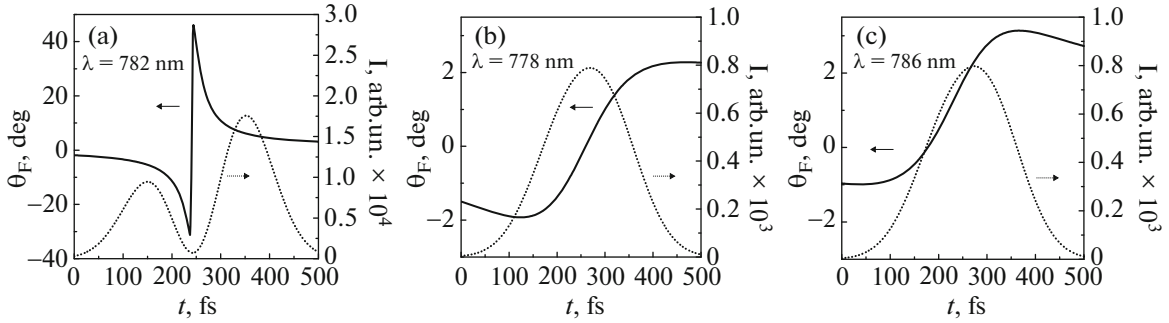

Fig. 2. Solid curves represent time dependences of Faraday rotation for wavelengths $\lambda =$ (a) 782, (b) 778, and (c) 786 nm. The dotted curves depict the intensities of the transmitted pulses.

and 786 nm. The dotted curves in Fig. 2 show the intensity profiles of the transmitted wave packet, the solid ones correspond to the Faraday rotation dynamics. If the central wavelength of the pulse coincides with the resonance wavelength $\lambda = 782$ nm, the original wave packet undergoes significant reshaping, splitting into two distinct pulses with durations of $\sim$120 fs each (see Fig. 2a). In this case, the polarization plane tilt within each pulse exhibits opposite signs, which means rotation in different directions. During the first part of the signal, the rotation is $\theta_F = -31°$, while for the second one it reaches $\theta_F = +46°$. Consequently, the polarizations of the first and second pulses are nearly orthogonal to each other, reaching the absolute rotation value of 77°. The use of a polarization beam splitter or a Glan prism after the magnetophotonic metasurface can separate the original single pulse into two orthogonally polarized pulses with durations half as long as the original pulse.

If the central wavelength of the laser pulse is tuned away from the exact resonance position, the shape of the transmitted pulse retains the original incident wave packet (Figs. 2b, 2c). The Faraday rotation varies slightly during the pulse increasing by 4° and also changing sign from $-1.9°$ to 2.1° for the carrier wavelength of 778 nm and from $-1°$ to 3° for the 786 nm.

The obtained dependences are attribute to the peculiarities of the local electromagnetic fields distribution inside the nanoparticle. The external magnetic field induces an additional phase shift between the field components, which eventually leads to large values of the Faraday rotation. It is found that the smaller the pulse duration, the larger the time derivative of the Faraday rotation. Conversely, in the limit of an infinitely long pulse or a continuous wave, the dynamics of the polarization plane rotation is absent, as the relative delay between the field components is fixed.

The currently known plasmonic structures, photonic crystals and other optical resonant structures give the Faraday rotation at the level of units of degrees and less, which limits their practical applicability [10, 16–23]. Subwavelength nanophotonic systems capable of achieving a 45° polarization rotation, as demonstrated in this work, have not been previously reported. Although the intensity of the transmitted pulse appears to be strongly suppressed, the linear nature of the effects discussed allows for the use of higher-power initial pulses to achieve the desired emission power after the magnetophotonic metasurface. An alternative way to increase the transmittance at the resonant wavelength could be the use of magnetic dielectrics. These could be nanostructured systems such as magnetophotonic crystals [22] or Mie-resonant metasurfaces [10]. It should be noted that the experimentally demonstrated Faraday rotation up to 14° has only been realized at cryogenic temperatures (20 K) under the excitation of propagating plasmon-polaritons in magnetic fields of 5 T [23].

CONCLUSIONS

The dynamics of Faraday rotation on the femtosecond scale is studied in Mie-resonant magnetophotonic metasurfaces formed by a two-dimensional array of silicon disks coated with a thin layer of nickel. The interference between the electric and magnetic dipole Mie resonances significantly enhances the polarization magneto-optical effect. In the static case, the maximal rotation of the polarization plane at the resonant wavelength reaches 14°. For femtosecond-scale effects, the incident wave packet is transformed into two orthogonally polarized wave packets, each with a duration that is half of the original signal. The simulation results in this study demonstrate the promising potential of metasurfaces for both magneto-optical applications and ultrafast optical processes. These findings can contribute to the development of new types of optical devices with improved dynamic magneto-optical properties.

FUNDING

This work is supported by the Russian Science Foundation (no. 20-12-00371, static spectra calculations) and the Foundation for the Development of Theoretical Physics and Mathematics "BASIS" (calculations of optical processes dynamics).

CONFLICT OF INTEREST

The authors of this work declare that they have no conflicts of interest.

REFERENCES

1. A. I. Kuznetsov, A. E. Miroshnichenko, M. L. Brongersma, Yu. S. Kivshar, and B. Luk'yanchuk, Science **354**, aag2472 (2016). https://doi.org/10.1126/science.aag2472
2. I. Staude, A. E. Miroshnichenko, M. Decker, N. T. Fofang, Sh. Liu, E. Gonzales, J. Dominguez, T. Sh. Luk, D. N. Neshev, I. Brener, and Yu. Kivshar, ACS Nano **7**, 7824 (2013). https://doi.org/10.1021/nn402736f
3. A. I. Kuznetsov, A. E. Miroshnichenko, Yu. H. Fu, J. Zhang, and B. Luk'yanchuk, Sci. Rep. **2**, 492 (2012). https://doi.org/10.1038/srep00492
4. A. B. Evlyukhin, S. M. Novikov, U. Zywietz, R. L. Eriksen, C. Reinhardt, S. I. Bozhevolnyi, and B. N. Chichkov, Nano Lett. **12**, 3749 (2012). https://doi.org/10.1021/nl301594s
5. P. D. Terekhov, K. V. Baryshnikova, Yu. A. Artemyev, A. Karabchevsky, A. S. Shalin, and A. B. Evlyukhin, Phys. Rev. B **96**, 35443 (2017). https://doi.org/10.1103/physrevb.96.035443
6. H. Hsiao, Ch. H. Chu, and D. P. Tsai, Small Methods **1**, 1600064 (2017). https://doi.org/10.1002/smtd.201600064
7. N. De Sousa, L. S. Froufe-Pérez, J. J. Sáenz, and A. García-Martín, Sci. Rep. **6**, 30803 (2016). https://doi.org/10.1038/srep30803
8. M. G. Barsukova, A. S. Shorokhov, A. I. Musorin, D. N. Neshev, Yu. S. Kivshar, and A. A. Fedyanin, ACS Photonics **4**, 2390 (2017). https://doi.org/10.1021/acsphotonics.7b00783
9. M. G. Barsukova, A. I. Musorin, A. S. Shorokhov, and A. A. Fedyanin, APL Photonics **4**, 16102 (2019). https://doi.org/10.1063/1.5066307
10. A. Christofi, Yu. Kawaguchi, A. Alù, and A. B. Khanikaev, Opt. Lett. **43**, 1838 (2018). https://doi.org/10.1364/ol.43.001838
11. P. Nuernberger, R. Selle, F. Langhojer, F. Dimler, S. Fechner, G. Gerber, and T. Brixner, J. Opt. A: Pure Appl. Opt. **11**, 085202 (2009). https://doi.org/10.1088/1464-4258/11/8/085202
12. A. I. Musorin, M. I. Sharipova, T. V. Dolgova, M. Inoue, and A. A. Fedyanin, Phys. Rev. Appl. **6**, 24012 (2016). https://doi.org/10.1103/physrevapplied.6.024012
13. G. S. Krinchik and V. A. Artem'ev, Sov. Phys. JETP **26**, 1080 (1968).
14. A. B. Evlyukhin, C. Reinhardt, and B. N. Chichkov, Phys. Rev. B **84**, 235429 (2011). https://doi.org/10.1103/physrevb.84.235429
15. Yu. Yang, I. I. Kravchenko, D. P. Briggs, and J. Valentine, Nat. Commun. **5**, 5753 (2014). https://doi.org/10.1038/ncomms6753
16. J. Ya. Chin, T. Steinle, T. Wehlus, D. Dregely, T. Weiss, V. I. Belotelov, B. Stritzker, and H. Giessen, Nat. Commun. **4**, 1599 (2013). https://doi.org/10.1038/ncomms2609
17. M. Kataja, T. K. Hakala, A. Julku, M. J. Huttunen, S. Van Dijken, and P. Törmä, Nat. Commun. **6**, 7072 (2015). https://doi.org/10.1038/ncomms8072
18. A. I. Musorin, A. V. Chetvertukhin, T. V. Dolgova, H. Uchida, M. Inoue, B. S. Luk'yanchuk, and A. A. Fedyanin, Appl. Phys. Lett. **115**, 151102 (2019). https://doi.org/10.1063/1.5124445
19. D. O. Ignatyeva, D. Karki, A. A. Voronov, M. A. Kozhaev, D. M. Krichevsky, A. I. Chernov, M. Levy, and V. I. Belotelov, Nat. Commun. **11**, 5487 (2020). https://doi.org/10.1038/s41467-020-19310-x
20. A. M. Chernyak, M. G. Barsukova, A. S. Shorokhov, A. I. Musorin, and A. A. Fedyanin, JETP Lett. **111**, 46 (2020). https://doi.org/10.1134/s0021364020010105
21. Sh. Xia, D. O. Ignatyeva, Q. Liu, H. Wang, W. Yang, J. Qin, Yi. Chen, H. Duan, Yi. Luo, O. Novák, M. Veis, L. Deng, V. I. Belotelov, and L. Bi, Laser Photonics Rev. **16**, 2200067 (2022). https://doi.org/10.1002/lpor.202200067
22. M. Inoue, R. Fujikawa, A. Baryshev, A. Khanikaev, P. B. Lim, H. Uchida, O. Aktsipetrov, A. Fedyanin, T. Murzina, and A. Granovsky, J. Phys. D: Appl. Phys. **39**, R151 (2006). https://doi.org/10.1088/0022-3727/39/8/r01
23. D. Floess, M. Hentschel, T. Weiss, H.-U. Habermeier, J. Jiao, S. G. Tikhodeev, and H. Giessen, Phys. Rev. X **7**, 21048 (2017). https://doi.org/10.1103/physrevx.7.021048